Journal of the Korean Physical Society (2022) 81:587–593
https://doi.org/10.1007/s40042-022-00405-1

Online ISSN 1976-8524
Print ISSN 0374-4884

ORIGINAL PAPER - ATOMS, MOLECULES AND OPTICS

Simulation study on the optical properties of hybrid films adopted in quantum-dot edge-lit backlights for LCD applications

Jung-Gyun Lee[1] · Gi Jung Lee[1] · Jae-Hyeon Ko[1]

Received: 7 September 2021 / Revised: 16 November 2021 / Accepted: 16 November 2021 / Published online: 22 March 2022

Abstract
A new hybrid optical film integrating several optical functions was adopted in a quantum-dot (QD) backlight for liquid crystal display applications. The hybrid film included two prism sheets and one reflective polarizer between which index-matching layers were inserted. The optical performances of the hybrid QD backlight were comparable to those of a conventional QD backlight where optical films were separately adopted. The on-axis luminance decreased slightly while the viewing angle became enhanced by adopting the hybrid film. The color gamut of the present hybrid QD backlight was more than 100% according to the National Television Standards Committee standard. The hybrid film suggested in this study can be used to reduce the number of optical films substantially and, thus, the fabrication process of backlights.

Keywords Quantum dot · Backlight · Hybrid film · LCD · Simulation

1 Introduction

Liquid crystal displays (LCDs) are the most widely used flat panel display in various applications [1]. Since LCD is a non-emissive display, it needs an additional lighting device called a backlight unit (abbreviated as BLU). The homogeneous, bright, white light supplied by BLU is modulated at the LCD panel to generate full-color images. BLU determines many optical performances of LCD, such as brightness, color gamut, and contrast ratio. Intensive efforts during the past decades have led to major technological innovations in LCD which became the major flat panel display dominating the market. One of these efforts has focused on the optical design of new backlight structures [2–10].

Traditional light sources in BLU have been white light-emitting diodes (LEDs) consisting of blue LED chips and color conversion materials [11, 12]. Yellow phosphors, such as YAG ($Y_3Al_5O_{12}$:Ce^{3+}) [13, 14], or the combination of red and green phosphors are the most conventional color conversion materials [15–22]. Recently, quantum dots (QDs) have been applied to BLU as new conversion materials to increase the color gamut of LCDs [23–25]. QDs are nanometer-sized semiconductor materials and are characterized by high color purity, color tunability due to the quantum confinement effect, and easy processibility [26–28]. The QD materials are fabricated as remote films to secure long-term stability [29].

BLU consists of many optical components, such as a reflection film, a light guide plate (LGP), a diffuser film, one or two collimation films, a reflective polarizer. The inclusion of QD films increases the number of optical films of BLU and, thus, the assembly time and the cost. In this context, the development of hybrid films or hybrid LGPs integrating several optical functions has been an important technological issue [30–35]. In our previous study, a new structure of a hybrid LGP where several optical films were integrated on the LGP was suggested [36]. Satisfactory optical properties including high uniformity were achieved from this structure. However, a low-index layer needs to be inserted between the LGP and other optical films, which is difficult to realize from the technological point of view. The purpose of this simulation study is to suggest an optical design of hybrid films which can be used to reduce the number of optical films adopted in BLU. Detailed optical characteristics of the hybrid films will be suggested and compared to the conventional design.

✉ Jae-Hyeon Ko
hwangkok@hallym.ac.kr

[1] School of Nano Convergence Technology, Nano Convergence Technology Center, Hallym University, Gangwon-do 24252, Korea

2 Simulation methods

A commercially available software LightTools (ver. 9.0.0, Synopsis Co.) was used for the simulation. Figure 1a shows a cross-sectional view of a conventional edge-lit backlight adopted in the simulation where a QD film is placed on the wedge-type LGP. The area of the LGP was 200×300 mm^2, and its thickness was changed from 3 (thicker part) to 1.25 (thinner part) mm. Total 38 blue LEDs were located on one of the side surfaces, the thicker part, and the total luminous flux was 500 lm. The LED showed a Gaussian spectrum at the center wavelength of 450 nm and a half-width of 20 nm. The side surfaces of the LGP were surrounded by reflection films with a diffuse Gaussian distribution of reflectance of 85% and angular width of 15°. The reflection film below the LGP was a simple mirror reflector having a reflectance of 95%. The material of the LGP was set to be polymethyl methacrylate (PMMA), and diffusing dots with a radius of 0.05 mm were formed on the bottom surface of the LGP for light homogenization.

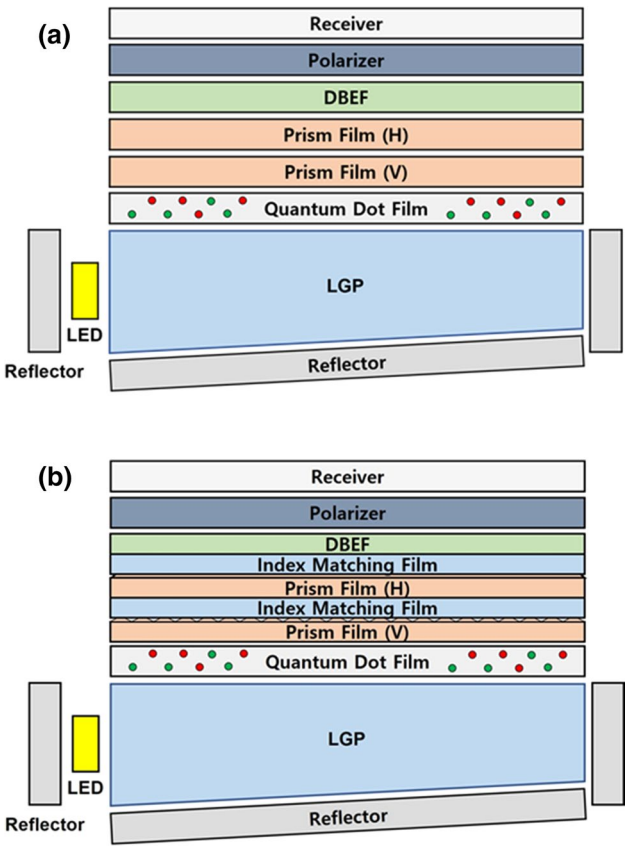

Fig. 1 Cross-sectional view of the backlight structure: **a** a conventional QD backlight and **b** an integrated QD backlight. The details are described in the text

The QD film includes red and green QDs, the mean free path (MFP) of which were 0.25 and 0.3 mm, respectively. The dimensions of the QD film were $200 \times 300 \times 0.1$ mm^3. The refractive index of the QD film was 1.5. The absorption and the emission spectra in addition to the quantum yield were adopted from reported values in a previous study [37]. The QD film plays the role of a diffuser film, thus no diffuser film was included in the simulation model. Two prism sheets (PSs) were put over the QD film. Each prism sheet consists of a substrate with a thickness of 0.127 mm and a refractive index of 1.59 and prism grooves with an apex angle of 90°, a refractive index of 1.667, and a pitch of 24 μm. The DBEF denotes the dual brightness enhancement film which is a multi-layer reflective polarizer [38]. Reflective polarization property was allocated to the upper and the lower surfaces of the DBEF using the built-in function of LightTools. In this case, the polarization component parallel to the transmission axis of the DBEF passes while the orthogonal component is reflected. The thickness of the DBEF was 0.1 mm and its refractive index was 1.5. Since the LCD panel was not considered in the model, an absorptive polarizer mimicking the bottom polarizer of the LCD panel was put over the BLU to characterize the polarization properties of the BLU.

Figure 1b shows the cross-section of the BLU where the hybrid film, which is suggested in this study, was adopted. To integrate three optical films (two PSs and one DBEF), two index-matching films (IMFs) with a thickness of 20 μm were inserted as shown in Fig. 1b. The thickness of the PS was slightly decreased to 0.105 mm to reduce the total thickness of the hybrid film. The material properties of the IMF were set to be those of PMMA. The prism grooves were immersed in the IMF with a thickness of 7 μm. Therefore, air remains between the prism grooves, which is important for maintaining the collimation function of the PS. This hybrid film will be denoted as "PSDBEF" which represents the combination of the PS and the DBEF. A flat luminance receiver with 21×21 meshes was used, and the typical number of rays used for the simulation was one million. Table 1 summarizes the physical parameters of the optical components included in the BLU models.

3 Results and discussion

To investigate the reliability of the polarization simulation for the DBEF, a conventional BLU without the QD film was studied by simulation in the first place. The simulation model was the same as that shown in Fig. 1a except for the fact that the QD film was replaced with a polycarbonate diffuser sheet (DS) having a thickness of 0.1 mm. The DS was modeled as a Gaussian diffuser with a spreading angle of 25°. Figure 2a shows the angular distribution of luminance on each film of the conventional backlight analyzed

Table 1 Physical parameters of the optical components and BLUs included in the simulation models

	Thickness or shape parameters	Refractive index
Light guide plate	200 mm × 300 mm × 3 mm	1.4936
Diffuser sheet	200 mm × 300 mm × 0.1 mm	1.5896
Quantum dot film	200 mm × 300 mm × 0.1 mm (red QD MFP 0.25 mm, green QD MFP 0.03 mm)	1.4936
Prism sheet (substrate)	200 mm × 300 mm × 0.127 mm	1.59
Prism sheet (prism groove)	200 mm × 300 mm × 0.012 mm	1.667
DBEF	200 mm × 300 mm × 0.1 mm	1.5
PSDBEF (total)	200 mm × 300 mm × 0.35 mm (DBEF + index-matching film × 2 + prism sheet × 2)	
Index matching film **(in** PSDBEF)	200 mm × 300 mm × 0.02 mm	1.4936
Prism sheet **(in** PSDBEF)	200 mm × 300 mm × 0.105 mm (substrate 0.093 mm, prism groove 0.012 mm)	Substrate 1.59 Prism groove 1.667
Polarizer	200 mm × 300 mm	
LED	2 mm × 1.3 mm × 0.5 mm (each 13.16 lm, total 500 lm)	
Reflector	200 mm × 300 mm × 0.1 mm	1.5

without the absorptive polarizer. The "None" case indicates the luminance distribution on the LGP, which is close to the Lambertian. The on-axis luminance on the DS is slightly modified and increased, which is consistent with experimental results [39]. The two PSs on the DS enhance the on-axis luminance significantly due to the refraction at the prism grooves combined with the angle recycling process [40]. For the light to be refracted toward the normal direction, the light should satisfy a certain angle range for its incidence. Approximately half of the light incident on the prism film is reflected via total internal reflections at the prism grooves toward the bottom of the BLU on which the light direction is changed significantly via diffuse reflection. This induces part of the reflected light to meet the condition of collimation via refraction at the prism grooves resulting in the luminance gain. This process is called "angle recycling". When the DBEF is put over the PS, the luminance decreases because part of the light is reflected due to the polarization selection function of the DBEF. However, the luminance on the LCD panel increases substantially when the DBEF is used thanks to the polarization recycling process [40]. The mechanism polarization recycling process is very similar to the angle recycling process. The only difference is that the polarization state of the reflected light from the DBEF toward the bottom of the BLU is partially changed due to the diffuse reflection, thus, part of the reflected light can pass through the DBEF resulting in the luminance gain. The overall luminance behaviors are consistent with previous simulation and experimental results [39].

Figure 2b shows the angular distribution of luminance on each film of the conventional backlight analyzed with a polarizer. The transmission axis of the absorptive polarizer was orthogonal to that of the DBEF. The overall distributions are nearly the same as those shown in Fig. 2a except for the fact that the luminance values decreased to approximately half due to the absorption by the absorptive polarizer and that the luminance on the DBEF is nearly zero due to the orthogonal transmission axes of the two polarizers. Then, the transmission axis of the absorptive polarizer was rotated by 90°, where it was parallel to that of the DBEF, and the same simulation was carried out. The result is shown in Fig. 2c. The luminance on DBEF has been increased due to the polarization recycling process consistent with the experiment [41–45], which demonstrates that the present simulation model is reliable. The difference in the luminance on the PS between (b) and (c) is attributed to the polarizing function of the prism grooves that is caused by the different Fresnel reflections of the s and p polarizations [41, 42].

As a next step, the QD BLU was investigated where the DS was replaced with a QD film as shown in Fig. 1a. In addition, the upper optical films (two PSs and the DBEF) were replaced by the hybrid film as shown in Fig. 1b. The former and the latter will be denoted as a conventional QD BLU and a hybrid QD BLU, respectively. Figure 3a shows the dependence of the luminance of each optical film of the conventional QD BLU on the angle of the transmission axis of the absorptive polarizer. The output light from the QD films is unpolarized as expected because there is no optical mechanism that polarizes the light. The luminance on each PS shows an oscillation behavior indicating that the emitted light from the PS is slightly polarized, consistent with experimental results [41, 42]. This is due to the Fresnel reflection at the prism grooves, i.e., the average reflectance of the s-polarization is higher than that of the orthogonal p-polarization [41, 42]. Since the prism grooves of the two PSs are orthogonal to each other, the oscillating luminance patterns on the two PSs are out of phase.

Figure 3b shows the dependence of the luminance of each optical film combined with the DBEF of the conventional

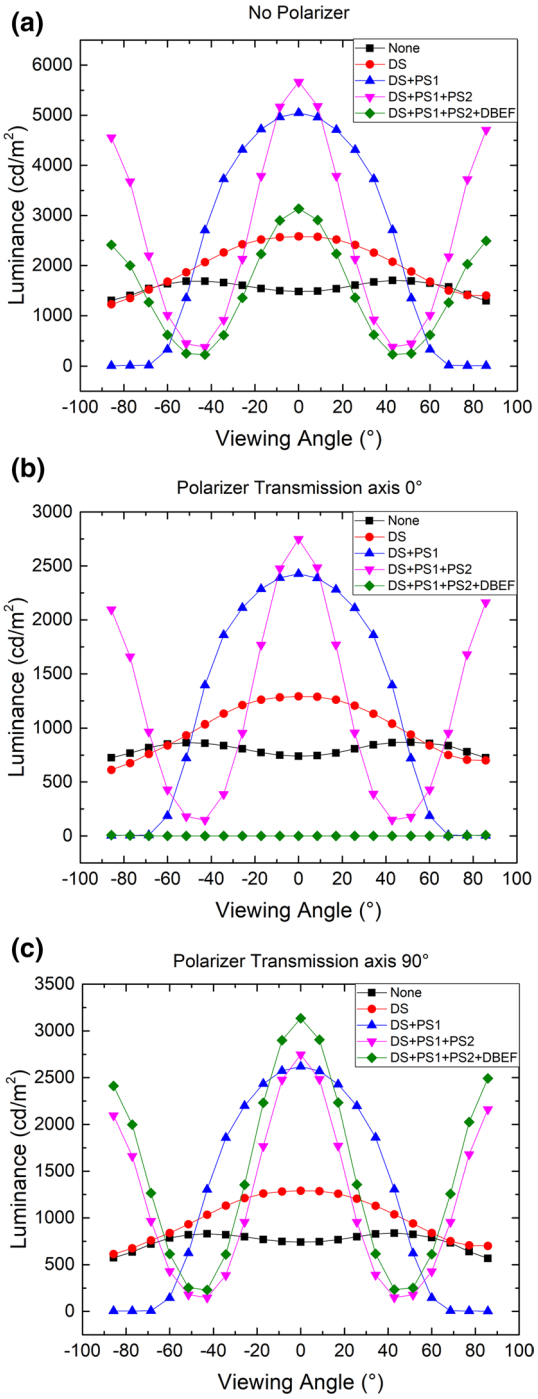

Fig. 2 Angular dependence of luminance on each optical film of **a** the conventional backlight without the absorptive polarizer, **b** with the absorptive polarizer whose transmission axis is orthogonal to that of the DBEF, and **c** with the absorptive polarizer whose transmission axis is parallel to that of the DBEF. "None" indicates the location on the LGP without any optical film

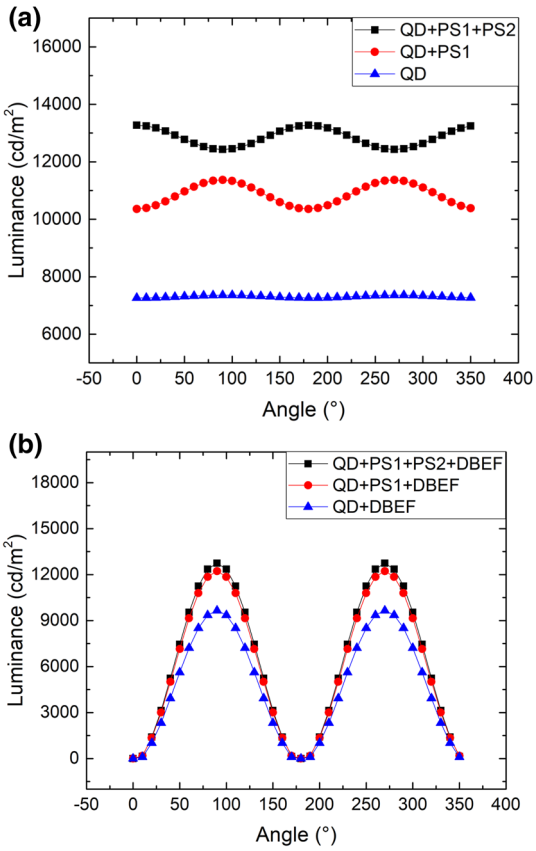

Fig. 3 The dependence of the luminance of each optical film **a** without and **b** with the DBEF of the conventional QD BLU on the angle of the transmission axis of the absorptive polarizer

QD backlight on the angle of the transmission axis of the absorptive polarizer. Depending on the angle between the transmission axes of the DBEF and the absorptive polarizer, the luminance shows an oscillating behavior with a period of 180°. The luminance becomes maximum and minimum when the two transmission axes are parallel and perpendicular to each other, respectively. The DBEF increases the maximum luminance on the QD film, QD + PS, and QD + PS + PS by 31.1%, 7.6%, and 2.6%, respectively. These relatively low luminance gains are partly due to the mirror reflector below the LGP and partly due to the absorption by the QD film. It is reported that the polarization recycling process of DBEF is facilitated when the downward rays are diffusely reflected efficiently [40–45].

Figure 4a shows the dependence of the luminance on the PSDBEF of the hybrid backlight on the angle of the transmission axis of the absorptive polarizer. Since the PSDBEF includes the reflective polarizer (DBEF), the luminance shows nearly the same oscillating behavior as that shown in Fig. 3b. Figure 4b shows the emitting spectrum of the hybrid backlight. It consists of a blue peak from the LEDs in addition to red and green peaks from QDs. The emitting spectrum of the conventional QD BLU is nearly the same as that shown in Fig. 4b. Relatively sharp spectral features are favorable for achieving a high

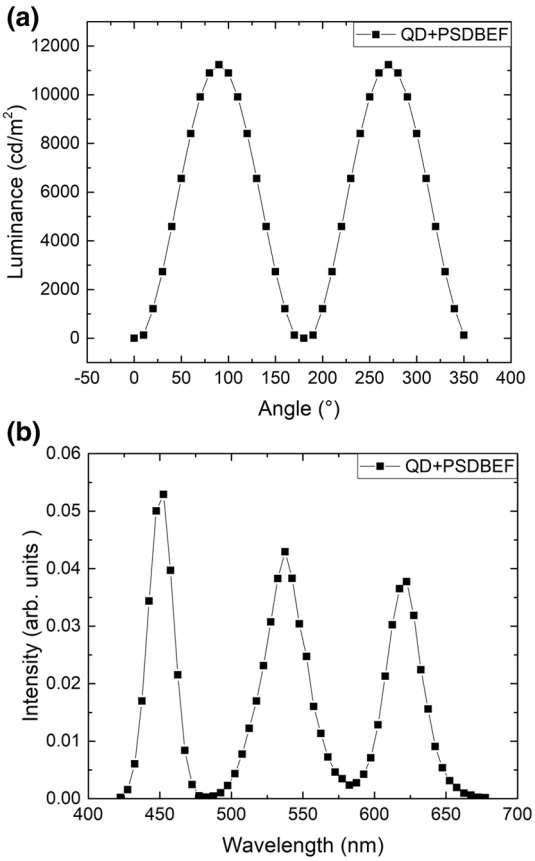

Fig. 4 **a** The dependence of the luminance of the hybrid QD BLU on the angle of the transmission axis of the absorptive polarizer. **b** The emitting spectrum of the hybrid QD BLU

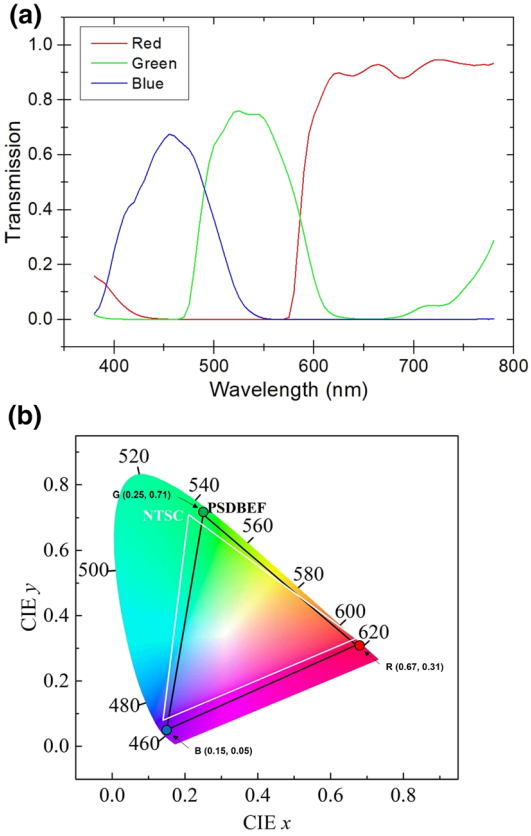

Fig. 5 **a** Transmission spectra of three color filters of a typical LCD panel. **b** The color gamut of the NTSC standard (white) and the hybrid QD BLU (black) on the CIE1931 chromaticity diagram. The color coordinates of the primary colors are included

color gamut of LCD. Figure 5a shows typical transmission spectra of color filters of LCD panels for TV applications. Figure 5b shows the chromaticity diagram on which the color gamut of the LCD combined with the hybrid QD backlight is compared to that of the National Television Standards Committee (NTSC) standard. The color gamut of this system is 100.3% according to the NTSC standard, which demonstrates the outstanding performance of the QD-based backlight from the viewpoint of color properties.

Figure 6a shows the angular dependence of luminance of the two backlights. The on-axis luminance of the conventional QD BLU is higher than that of the hybrid QD BLU. However, the luminance distribution of the hybrid QD BLU is broader. In the case of the conventional QD BLU, the two PSs contribute to the collimation in their full performances. However, the apex part of the prism grooves of the PSs in the hybrid film was immersed in the IMFs, which decreases the collimating ability of the PS resulting in lower on-axis luminance. However, the wider angular distribution of luminance is preferable in some applications due to the better viewing-angle performances.

Figure 6b shows the change in the color coordinates (x, y) of the QD backlights depending on the configuration of optical films. The color coordinates on the QD film are located in the blue-shifted region indicating insufficient color conversion via QDs. As other optical films are put on the QD film in turn, the color coordinates shift to higher values sequentially. In the case of a PS, approximately half of the incident light is reflected due to the total internal reflection at the prism grooves. In addition, the DBEF reflects the light with the polarization direction perpendicular to its transmission axis, which comprises ~ 50% of the incident light. These downward rays will undergo multiple passages through QD films contributing to the color conversion. In the case of the hybrid QD BLU, the color coordinates are close to those of the conventional QD BLU. This suggests that enough color conversion occurs via the PSs and DBEF integrated into the hybrid film.

The present simulation study demonstrates that multiple optical functions played by several optical films included in the conventional BLU can be integrated into one hybrid film without any substantial degradation of performances. The on-axis luminance decreased slightly,

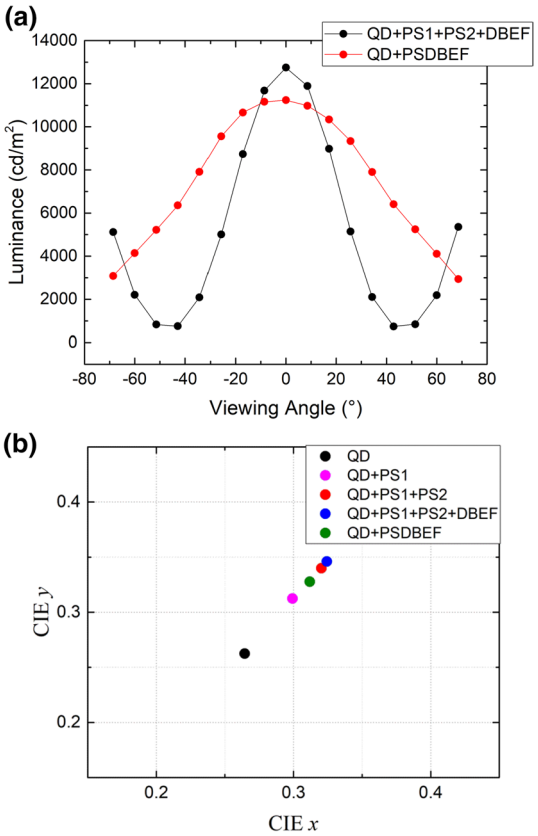

Fig. 6 **a** Angular dependence of luminance of the conventional QD BLU and the hybrid QD BLU. **b** The color coordinates of the conventional QD BLU under different optical configurations and those of the hybrid QD BLU

but the viewing-angle property was improved. In addition, it was found that the integrated optical films could cause enough color conversion via appropriate reflections. The estimated color gamut of the LCD with the hybrid QD BLU was larger than 100% compared to the NTSC standard. This approach of using the hybrid film in BLUs can be adopted to make the fabrication process of BLU simpler due to much smaller number of optical components. Further optimization may be possible when the QD film is incorporated into the hybrid film.

Finally, it should be indicated that the viewing angle and the on-axis luminance form a trade-off relationship. If the on-axis luminance increases, the viewing-angle decreases, vice versa. One way to increase the on-axis luminance is to adjust and optimize the refractive index of the prism grooves, as well as the refractive index of the index-matching layer. The on-axis luminance is expected to increase as the refractive index of the grooves increases. In this case, however, the viewing angle will decrease due to the high collimation toward the normal direction.

4 Conclusion

Two prism sheets and one reflective polarizer (DBEF), typically used in conventional backlights, were integrated into one hybrid film, which was adopted in a QD BLU. The on-axis luminance of the hybrid QD BLU was lower compared to that of the conventional QD BLU, which is attributed to the worse collimating performance of prism sheets the apex of which was partly immersed in the index-matching layer. However, the viewing-angle property became better which is favorable for many applications where several people watch the display screen from different viewing directions. The color gamut of the hybrid QD BLU was more than 100% according to the NTSC standard. The present approach can be used to innovate the backlight fabrication process due to the much smaller number of optical components assembled in the backlight.

Acknowledgements This research was supported by the Ministry of Trade, Industry and Energy (MOTIE), Korea Institute for Advancement of Technology (KIAT) through the program of Smart Specialized Infrastructure Construction (no. P0013743).

References

1. P. Yeh, C. Gu, *Optics of liquid crystal displays*, 2nd edn. (Wiley, New York, 2009)
2. M. Tjahjadi, G. Hay, D.J. Coyle, E.G. Olczak, Inf. Display **10**(06), 22 (2006)
3. K. Kakinuma, Jpn. J. Appl. Phys. **45**, 4330 (2006)
4. J.-H. Lee, H.-S. Lee, B.-K. Lee, W.-S. Choi et al., Opt. Lett. **32**, 2665 (2007)
5. I. Kim, K. Chung, J. Opt. Soc. Korea **11**, 67 (2007)
6. J. Jeong, J. Kim, M. Shin, M. Lee, J. Chung et al., J. Korean Vac. Soc. **16**, 424 (2007)
7. G.-J. Park, Y.-G. Kim, J.-H. Yi, J.-H. Kwon et al., J. Opt. Soc. Korea **13**, 152 (2009)
8. G. Park, T.S. Aum, J.H. Kwon, J.H. Park, B.K. Kim et al., J. Korean Phys. Soc. **54**, 44 (2009)
9. S.-T. Hur, S.-W. Choi, M. Lee, J. Korean Phys. Soc. **58**, 392 (2011)
10. B.-Y. Joo, J.-H. Ko, Curr. Opt. Photonics **1**, 101 (2017)
11. E.F. Schubert, J.K. Kim, H. Luo, J.-Q. Xi, Rep. Prog. Phys. **69**, 3069 (2006)
12. T. Taki, M. Strassbug, ECS J. Solid State Sci. Technol. **9**, 015017 (2020)
13. S. Nishiura, S. Tanabe, K. Fujioka, Y. Fujimoto, Opt. Mater. **33**, 688 (2011)
14. H.-W. Choi, J.-H. Ko, Korean J. Opt. Photonics **24**, 64 (2013)
15. L. Wang, X. Wang, T. Kohsei, K. Yoshimura, M. Izumi et al., Opt. Express **23**, 28707 (2015)
16. J.H. Oh, H. Kang, M. Ko, Y.R. Do, Opt. Express **23**, A791 (2015)
17. L.-L. Wei, C.C. Lin, Y.-Y. Wang, M.-H. Fang, H. Jiao et al., ACS Appl. Mater. Interfaces **7**, 10656 (2015)
18. W.-L. Wu, M.-H. Fang, W. Zhou, T. Lesniewski, S. Mahlik et al., Chem. Mater. **29**, 935 (2017)
19. D. Luo, L. Wang, S. Wing Or, H. Zhang, R.-J. Xie, RSC Adv. **7**, 25964 (2017)

20. M. Kim, W.B. Park, B. Bang, C.H. Kim, K.-S. Sohn, J. Mater. Chem. C **3**, 5484 (2015)
21. D.Y. Jeong, J. Ju, D.H. Kim, New Phys. Sae Mulli **66**, 311 (2016)
22. J.S. Park, S.J. Kim, M. Jang, J.-H. Ko, New Phys. Sae Mulli **69**, 410 (2019)
23. Z. Luo, Y. Chen, S.-T. Wu, Opt. Express **21**, 26269 (2013)
24. E. Jang, S. Jun, H. Jang, J. Lim, B. Kim, Y. Kim, Adv. Mater. **22**, 3076 (2010)
25. S. Abe, J.J. Joos, L.I.D.J. Martin, Z. Hens, P.F. Smet, Light Sci. Appl. **6**, e16271 (2017)
26. D. Bera, L. Qian, T.-K. Tseng, P.H. Holloway, Materials **3**, 2260 (2010)
27. H.V. Demir, S. Nizamoglu, T. Erdem, E. Mutlugun, N. Gaponik, A. Eychmüller, Nano Today **6**, 632 (2011)
28. M.J. Anc, N.L. Pickett, N.C. Gresty, J.A. Harris, K.C. Mishra, ECS J. Solid State Sci. Technol. **2**, R3071 (2013)
29. S.J. Kim, H.W. Jang, J.-G. Lee, J.-H. Ko, Y.W. Ko, Y. Kim, New Phys. Sae Mulli **69**, 861 (2019)
30. T. Okumura, A. Tagaya, Y. Koike, M. Horiguchi, H. Suzuki, Appl. Phys. Lett. **83**, 2515 (2003)
31. X. Yang, Y. Yan, G. Jin, Appl. Phys. Lett. **88**, 221109 (2006)
32. S.R. Park, O.J. Kwon, D. Shin, S.-H. Song, H.-S. Lee, H.W. Choi, Opt. Express **15**, 2888 (2007)
33. J.-H. Lee, H.-S. Lee, B.-K. Lee, W.-S. Choi, H.-Y. Choi, J.-B. Yoon, Opt. Lett. **32**, 2665 (2007)
34. E.S. Choi, Y.H. Choi, Y.J. Shin, J. Korean Phys. Soc. **55**, 2646 (2009)
35. H.J. Jeon, J.S. Gwag, J.H. Kwon, Korean J. Opt. Photonics **30**, 101 (2019)
36. J.-G. Lee, J.-H. Ko, J. Korean Phys. Soc. **77**, 264 (2020)
37. M.H. Shin, H.-J. Kim, Y.-J. Kim, Opt. Express **25**, A113 (2017)
38. M.F. Weber, C.A. Stover, L.R. Gilbert, T.J. Nevitt, A.J. Ouderkirt, Science **287**, 2451 (2000)
39. Y.H. Ju, J.-H. Park, J.H. Lee, J.-Y. Lee, K.-B. Nahm et al., J. Opt. Soc. Korea **12**, 25 (2008)
40. P. Watson, G.T. Boyd, in *Mobile displays*, ed. by A. K. Bhowmik et al. Chap. 7 (Wiley, Atrium, 2008), pp. 211–225
41. M.-Y. Yu, B.-W. Lee, J.H. Lee, J.-H. Ko, J. Opt. Soc. Korea **13**, 256 (2009)
42. B.-W. Lee, M.-Y. Yu, J.-H. Ko, J. Inf. Disp. **10**, 28 (2009)
43. J.S. Seo, T.E. Yeom, J.-H. Ko, J. Opt. Soc. Korea **16**, 151 (2012)
44. S.H. Jeong, A. Park, S.J. Kim, D.J. Park, J.-H. Ko, New Phys. Sae Mulli **69**, 101 (2019)
45. G.J. Lee, J.-G. Lee, Y. Kim, T. Park, Y.W. Ko et al., J. Inf. Disp. **22**, 55 (2021)